Polymer Chemistry

Directing Network Degradability Using Wavelength-Selective Thiol-Acrylate Photopolymerization

Journal:	*Polymer Chemistry*
Manuscript ID	PY-ART-11-2023-001285.R1
Article Type:	Paper
Date Submitted by the Author:	29-Jan-2024

Complete List of Authors:	Alfarhan, Saleh; Arizona State University - Tempe Campus, Chemical Engineering, School for Engineering of Matter, Transport and Energy Nettles, Jared; Arizona State University - Tempe Campus, Chemical Engineering, School for Engineering of Matter, Transport and Energy; Arizona State University - Tempe Campus, Biodesign Center for Sustainable Macromolecular Materials and Manufacturing Prabhudesai, Parimal; Arizona State University - Tempe Campus, Mechanical Engineering, School for Engineering of Matter, Transport and Energy Yu, Jen-Chieh; Arizona State University - Tempe Campus, Chemical Engineering, School for Engineering of Matter, Transport, and Energy; Arizona State University - Tempe Campus, Biodesign Center for Sustainable Macromolecular Materials and Manufacturing Westover, Clarissa; Arizona State University - Tempe Campus, Biodesign Center for Sustainable, Macromolecular Materials and Manufacturing; Arizona State University - Tempe Campus, Materials Science and Engineering, School for Engineering of Matter, Transport and Energy Tang, Tengteng; Arizona State University - Tempe Campus, Mechanical Engineering, School for Engineering of Matter, Transport and Energy Wang, Wenbo; Arizona State University, School of Manufacturing Systems and Networks Chen, Xiangfan; Arizona State University, School of Manufacturing Systems and Networks Seo, Soyoung; Arizona State University - Tempe Campus, Chemical Engineering, School for Engineering of Matter, Transport and Energy; Arizona State University - Tempe Campus, Biodesign Center for Sustainable Macromolecular Materials and Manufacturing Li, Xiangjia; Arizona State University - Tempe Campus, Mechanical Engineering, School for Engineering of Matter, Transport and Energy Long, Timothy; Arizona State University - Tempe Campus, Biodesign Center for Sustainable Macromolecular Materials and Manufacturing; Arizona State University - Tempe Campus, Chemistry, School of Molecular Sciences; Arizona State University - Tempe Campus, Chemical Engineering, School for Engineering of Matter, Transport and Energy Jin, Kailong; Arizona State University - Tempe Campus, Chemical Engineering, School for Engineering of Matter, Transport and Energy; Arizona State University - Tempe Campus, Biodesign Center for Sustainable Macromolecular Materials and Manufacturing

Directing Network Degradability Using Wavelength-Selective Thiol-Acrylate Photopolymerization

Saleh Alfarhan,[a] Jared Nettles,[a,b] Parimal Prabhudesai,[c] Jen-Chieh Yu,[a,b] Clarissa Westover,[b,d] Tengteng Tang,[c] Wenbo Wang,[e] Xiangfan Chen,[e] Soyoung E. Seo,[a,b] Xiangjia Li,[c] Timothy Long,[a,b,f] and Kailong Jin[a,b,*]

[a]*Chemical Engineering, School for Engineering of Matter, Transport and Energy, Arizona State University, Tempe, AZ 85287, USA*

[b]*Biodesign Center for Sustainable Macromolecular Materials and Manufacturing, Arizona State University, Tempe, AZ 85287, USA*

[c]*Mechanical Engineering, School for Engineering of Matter, Transport and Energy, Arizona State University, Tempe, AZ 85287, USA*

[d]*Materials Science and Engineering, School for Engineering of Matter, Transport and Energy, Arizona State University, Tempe, AZ 85287, USA*

[e]*School of Manufacturing Systems and Networks (MSN), Arizona State University, Mesa, AZ 85212, USA*

[f]*Chemistry, School of Molecular Sciences, Arizona State University, Tempe, AZ 85287, USA*

*****To whom correspondence should be addressed: kailong.jin@asu.edu*

Abstract

Wavelength-selective photopolymerization employs light at controlled wavelengths to trigger orthogonal photochemical reactions to fabricate multimaterials with unique combinations of building blocks and material properties. Prior wavelength-selective photopolymerization studies mainly focused on modulating the thermomechanical properties of the resulting multimaterials, which are often permanently crosslinked, non-degradable polymer networks. Here, we combine

wavelength-selective photopolymerization with dynamic covalent chemistry to fabricate multimaterials with programmable, stimuli-responsive degradability in selected regions. Specifically, this study employs a thiol-acrylate photoresin comprising both wavelength-selective photoinitiators/photosensitizers and dynamic disulfide bonds. Green light irradiation triggers photobase generators to catalyze the thiol-acrylate Michael addition reactions, forming a step-growth polymer network with dynamic disulfide bond-based crosslinks. This green light-cured network can subsequently undergo degradation/decrosslinking by reacting with excess reactive thiols through thiol-disulfide exchange reactions. Meanwhile, UV light irradiation cleaves radical photoinitiators and thus promotes both radical-mediated acrylate homopolymerization and thiol-acrylate addition reactions, forming a permanently crosslinked chain-growth network that cannot be degraded. Promisingly, this thiol-acrylate photoresin can undergo orthogonal wavelength-selective photopolymerization under patterned green- and UV-light irradiation to form crosslinked multimaterials with pre-designed degradable regions, which can be selectively removed to reveal the underlying photomasks' patterns. Overall, the chemistry demonstrated herein can be used to fabricate complex patterns and hierarchical structures, holding promise for applications ranging from photolithography to 3D printing.

1. Introduction

Wavelength-selective photopolymerization involves the use of irradiation light at controlled wavelengths to trigger photoinitiators or photosensitizers that can subsequently promote distinct photochemical reaction pathways in an orthogonal manner.[1-5] Due to its wavelength selectivity and spatiotemporal control, wavelength-selective photopolymerization is capable of

fabricating complex polymeric materials or multimaterials with unique combinations of properties for advanced chemical and biological applications.[6, 7] For example, wavelength-selective photopolymerization has been used to incorporate various building blocks and functionalities into a single polymeric matrix, including thiol-ene/thiol-epoxy,[8-10] epoxy/acrylate,[11-15] thiol-acrylate/acrylate,[16-18] and many other hybrid systems.[19-33]

Wavelength-selective photopolymerization can fabricate these multimaterials through both simultaneous and sequential polymer network formations.[8-33] For example, Hawker and coworkers employed photochromic dyes to enable wavelength-selective photopolymerization of a hybrid epoxy/acrylate resin and successfully 3D printed a multimaterial comprising patterned rigid and soft domains in a single step.[12] In that study, the rigid domains formed under blue light irradiation where simultaneous cationic epoxy and radical-based acrylate homopolymerization occurred, while the soft domains formed under green light irradiation where only radical-based acrylate homopolymerization occurred.[12] In another example, Zhang et al. demonstrated a two-stage photopolymerization process controlled sequentially by visible and UV light for a nonstoichiometric thiol-acrylate photoresin having an excess of acrylate monomers.[17] In the first stage, visible light irradiation triggered a photobase generator to release a strong base that catalyzed the stoichiometric anion-mediated thiol-acrylate Michael addition reactions.[34, 35] In the second stage, UV light irradiation promoted a radical-mediated reaction pathway through which the unreacted acrylates in the system underwent acrylate homopolymerization, resulting in an increase in the final polymer network's crosslink density.[17]

Prior wavelength-selective photopolymerization studies have primarily focused on modulating the thermomechanical properties of the resulting hybrid multimaterials, which are often permanently crosslinked, non-degradable polymer networks.[3] It would be attractive if one

could use wavelength-selective photopolymerization to incorporate unique functionalities (e.g., stimuli-responsive behavior) into these multimaterials in a programmable manner. Herein, we focus on combining wavelength-selective photopolymerization with dynamic covalent chemistry[36-47] to impart stimuli-responsive degradability into specific regions of the resulting multimaterials. In our previous study, we developed degradable crosslinked thiol-ene photopolymers that contain dynamic disulfide bonds from commercially available building blocks including Thioplast G4, a reactive difunctional thiol comprising internal disulfide bonds.[48] The incorporated dynamic disulfide bonds allow these dynamically crosslinked thiol-ene photopolymers to undergo degradation/decrosslinking through base-catalyzed thiol-disulfide exchange reactions with excess reactive thiols.[48-50] The resulting disulfide-containing reactive thiol oligomers can be reused to form next-generation degradable thiol-ene networks with nearly identical material properties and chemical recyclability.[48]

In this study, we develop a thiol-acrylate photoresin which comprises dynamic disulfide bonds and can undergo orthogonal wavelength-selective photopolymerization for fabricating multimaterials with programmed degradability in specific regions. Specifically, we use a green light photobase generator to catalyze the thiol-acrylate Michael addition reactions to form a degradable step-growth network comprising dynamic disulfide bond-based crosslinks under green light irradiation (**Scheme 1**). This network can be later deconstructed/degraded by excess reactive thiols through thiol-disulfide exchange reactions. Simultaneously, we use a UV light radical photoinitiator to promote radical-mediated reaction pathways, including both acrylate homopolymerization (dominant) and thiol-acrylate addition (minor) reactions (**Scheme 1**).[51] Such a dominant acrylate homopolymerization reaction pathway under UV light irradiation results in a chain-growth network that is permanently crosslinked and thus cannot be degraded. Its unique

wavelength-selective characteristic allows this thiol-acrylate photoresin to undergo programmable curing under photomasked green- and UV-light irradiation to form crosslinked multimaterials with pre-designed degradable regions (i.e., green light-irradiated regions). The as-cured multimaterials show a continuous and smooth surface that is visually featureless. After selectively degrading the green light-irradiated regions in these multimaterials, the rest UV light-cured regions remain, thus revealing the underlying photomasks' patterns (e.g., a "butterfly shape). These new photoresins with unique wavelength-programmable degradability hold promise for creating complex photopatterns with intricate designs as well as 3D printing hierarchically structured materials with internal voids/channels.

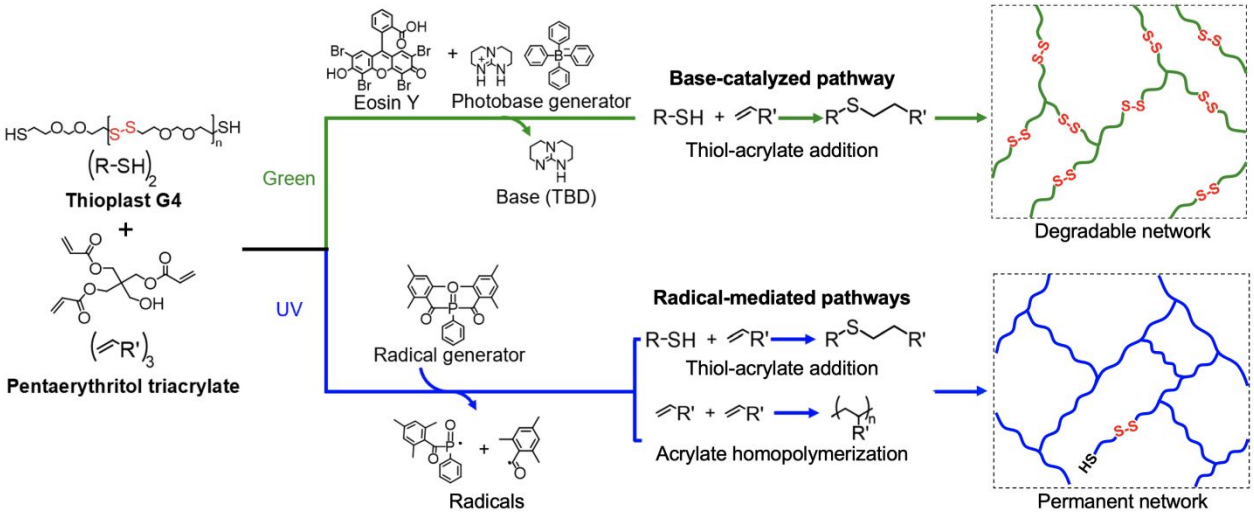

Scheme 1. Schematic illustration of the thiol-acrylate photoresin in this study undergoing orthogonal wavelength-selective photopolymerization reactions after irradiating with green light (i.e., base-catalyzed) *vs.* UV light (i.e., radical-mediated) to produce a degradable dynamic *vs.* a non-degradable permanent polymer network.

2. Experimental

2.1. Materials and Methods.

2.1.1. Materials. Pentaerythritol triacrylate (technical grade), triethylamine (99.5%), 1,5,7-triazabicyclo[4.4.0]dec-5-ene (TBD; 98%), sodium tetraphenylborate ($NaBPh_4$; 99.5%), Eosin Y (green light photosensitizer; 99%), 2,2,6,6-tetramethylpiperidine-1-oxyl (TEMPO; 98%),

hydrochloric acid (HCl; 37 wt% aqueous solution), and chloroform-d ($CDCl_3$; 99.8%) were purchased from Sigma-Aldrich. Thioplast G4 (a difunctional thiol which contains ~5 disulfide bonds on average in its backbone; $M_w \approx 980$ g mol^{-1}) was kindly donated to us by Nouryon. UV light photoinitiator (Omnirad 2100) was kindly donated to us by IGM resins. Acetone (99.5%) was purchased from Oakwood Chemical.

2.1.2. Synthesis of photobase generator (triazabicyclodecane tetraphenylborate; TBD-HBPh$_4$). The TBD-HBPh$_4$ synthesis followed a previous protocol reported by Sun et al.[52] Specifically, TBD (~1.4 g, ~10 mmol) was first dissolved in 10 wt% HCl (10 mL, ~27.4 mmol) aqueous solution, to which an aqueous solution comprising $NaBPh_4$ (~3.8 g, ~11 mmol) and 10 mL DI water was added dropwise.[52] The precipitated salt was filtered and washed with DI water twice and then with methanol once.[52] Finally, the salt was recrystallized from a methanol/chloroform mixture (4:1 by volume) at 70 ^oC, followed by filtration and vacuum drying to yield a white crystalline solid, i.e., TBD-HBPh$_4$ photobase generator (**Figure S1** in **Supporting Information**).[52]

2.1.3. Photoresin preparation. The thiol-acrylate photoresins in this study had a 1:1 stoichiometric ratio between thiol [SH] and acrylate [C=C] functional groups. Specifically, a typical photoresin contains ~5 g Thioplast G4 (~5.1 mmol, ~10.2 mmol [SH] groups, and ~25.5 mmol disulfide [S-S] bonds) and ~1.3 g triacrylate (~3.4 mmol, ~10.2 mmol [C=C] groups) monomers. The monomer mixture was then combined with 0.25 wt% Eosin Y, 1 wt% TBD-HBPh$_4$, 3 wt% Omnirad 2100, and 3 wt% TEMPO. (Note: All these wt% loadings are relative to the total weight of Thioplast G4 and triacrylate.) Excess acetone was introduced to achieve a homogeneous solution which was then extracted via rotary evaporation and vacuum drying at room temperature. The resulting photoresin appeared homogeneous and red in color.

2.1.4. Photoresin curing. To obtain single-layer films for testing, the thiol-acrylate photoresins were casted between two glass slides with 0.5-mm-thick spacers. The sandwiched photoresins then underwent two separate curing processes at room temperature, one under UV light and the other under green light. For UV curing, the photoresin was irradiated by a UV light source (Omnicure s1500 coupled with a 329–500 nm wavelength optical filter; ~95% of the photon energy of the filtered light is between 329–450 nm) at 50 mW cm^{-2} for 6 min (3 min per side). For green light curing, the photoresin was irradiated by a green light source (Kessil PR-160L-525 nm, whose emission light is between ~500–570 nm) at 80 mW cm^{-2} for 15 min (7.5 min per side).

To obtain photopatterned films, a homemade multiwavelength vat photopolymerization-based 3D printer was constructed. Specifically, a digital light processing (DLP) projector with a 405 nm light source (MoonRay S100; SprintRay *Inc*.) was used to generate a UV light pattern at an intensity of ~10 mW cm^{-2} for 30 min. The projector's UV light was directed through a 150 mm focal length biconvex lens (LB1437-A-ML, Thorlabs *Inc*.) and then a beam splitter (CCM1-BS013, Thorlabs *Inc*.) to the building platform. The building platform has a print area of 24.5 × 18.4 mm onto which patterned images (i.e., an "ASU" logo and a "butterfly" shape) with a resolution of 1024 × 768 pixels were projected. After patterned UV light irradiation, the whole film (including both UV-cured and uncured regions) was irradiated with green light (Kessil PR-160L-525 nm) at 80 mW cm^{-2} for 15 min to achieve photopatterned films.

2.1.5. Degradation of green light-cured photoresins via thiol-disulfide exchange. Complete decrosslinking of the green light-cured photoresins was achieved by base-catalyzed thiol-disulfide exchange reactions.[48] Typically, ~0.5 g of the green light-cured thiol-acrylate films (~2 mmol [S-S]) was shredded into small pieces to fit in a 20 mL vial, to which ~2 g of Thioplast G4 (~2 mmol, ~4 mmol [SH], ~10 mmol [S-S]), ~0.4 g of triethylamine (~4 mmol), and ~10 mL of acetone were

added. The resulting mixture was stirred overnight at room temperature to undergo network deconstruction via base-catalyzed thiol-disulfide exchange reactions.[48] After ~6 h, a homogeneous solution was obtained, which was then concentrated by rotary evaporation and vacuum dried at room temperature for 24 h to fully remove the volatile triethylamine and acetone.

Similarly, the photopatterned film (each ~0.5 g) on a glass substrate was immersed in a solution containing 10 mL of acetone, ~2 g of Thioplast G4 (~2 mmol, ~4 mmol [SH], ~10 mmol [S-S]), and ~0.4 g of triethylamine (~4 mmol) at room temperature. This process selectively degraded the green light-cured regions in a manner similar to the degradation procedure described above. After fully degrading the green light-cured regions, the photopatterned films left on the glass substrates were rinsed with acetone and then vacuum dried at room temperature for 24 h.

2.2. Characterizations

2.2.1. Ultraviolet-visible (UV-vis) absorption spectroscopy. A series of solutions containing Eosin Y, TBD-$HBPh_4$, Omnirad 2100, and photoresin in acetonitrile were prepared. Eosin Y, TBD-$HBPh_4$, and Omnirad 2100 solutions had a concentration of 4×10^{-6} mol L^{-1}, whereas the photoresin solution had a concentration of 2×10^{-3} mol L^{-1}. The light absorbance of each solution was measured using a Cary 3500 UV-Vis spectrophotometer.

2.2.2. Proton nuclear magnetic resonance (^{1}H NMR). The ^{1}H NMR spectra of TBD-$HBPh_4$, photoresin, and decrosslinked materials were obtained using a Bruker Avance NEO 500 MHz NMR. The sample concentration was ~5% (w/v) in $CDCl_3$.

2.2.3. Attenuated total reflectance Fourier transform infrared spectroscopy (ATR-FTIR). ATR-FTIR spectra of these thiol-acrylate photoresins before, during, and after curing were collected on a Nicolet iS10 spectrometer. Each spectrum had an average of ~15 scans over a 4000–

400 cm^{-1} wavenumber range. All these FTIR spectra were normalized to the unchanging absorbance peak at 1023 cm^{-1}, which is assigned as the C-O stretching band.[53]

2.2.4. Photo-rheological measurements. Photo-rheological measurements were performed on a Discovery HR 30 rheometer with a UV-curing accessory and a 20-mm-diameter parallel plate. A strain of 0.1%, a frequency of 1 Hz, and a gap of 0.5 mm were applied on each sample. The UV irradiation at an intensity of 50 mW cm^{-2} was initiated after 30 seconds into the rheological run. The UV light was transmitted from an Omnicure s2000 lamp (250–450 nm wavelength range) with a light guide onto a quartz parallel plate.

2.2.5. Gel weight fraction determination. In a typical gel fraction determination, ~0.2 g of a crosslinked thiol-acrylate film was immersed in excess acetone in a 20 mL vial to swell for ~24 h. Acetone was then carefully removed using a glass pipette, and fresh acetone was added to the swollen film. This process was repeated three additional times prior to vacuum drying the swollen film at room temperature. The gel fraction was determined by comparing the weights of the original thiol-acrylate film and the dried film after extraction.

2.2.6. Differential scanning calorimetry (DSC) test. DSC measurements were performed using a TA Instruments DSC 2500 under N_2 atmosphere. Each DSC experiment involved loading ~4–5 mg of sample into a hermetically sealed aluminum pan. The samples were initially heated to 120 ^oC at 10 ^oC min^{-1} to erase thermal history. Subsequently, the samples were quenched down to -80 ^oC and then heated to 120 ^oC at 10 ^oC min^{-1} to determine the glass transition temperature (T_g). All T_g values are reported from the second heating cycle.

2.2.7. Thermogravimetric analyses (TGA) test. TGA experiments were conducted using a TA Instruments TGA 5500. ~4 mg of each sample was heated to 600 ^oC at 10 ^oC min^{-1} under N_2 atmosphere.

2.2.8. Determination of tensile properties. Tensile tests were conducted on an Instron 3343 equipped with a 100 N load cell. ASTM D1708 dog-bone-shaped specimens (15mm × 5 mm × 0.5 mm) were punched out of the cured film samples. These specimens were then subjected to tensile tests at a strain rate of 1 mm min^{-1}. Tensile tests on each sample were repeated at least four times, allowing for the calculation of both average properties and standard deviations based on the obtained data.

2.2.9. Scanning electron microscopy (SEM). SEM characterization was performed on a Phenom XL G2 instrument. Prior to SEM characterization, the samples were coated with ~6 nm of gold using a LUXOR sputter coater. SEM analysis was conducted with an accelerating voltage of 15 kV under high-pressure vacuum conditions (0.1 Pa) by a backscattered electron detector.

3. Results and Discussion

The thiol-acrylate photoresin in this study (**Scheme 1**) is comprised of disulfide-bearing difunctional thiol (Thioplast G4), trifunctional acrylate, UV-light radical photoinitiator (Omnirad 2100), green-light photosensitizer (Eosin Y), photobase generator (TBD-$HBPh_4$), and radical scavenger (TEMPO). A stoichiometric balance between thiol [SH] and acrylate [C=C] functional groups was maintained in this thiol-acrylate photoresin, as confirmed by ^{1}H NMR (see **Figure S2** in **Supporting Information** for more details).

Omnirad 2100 and Eosin Y are chosen because of their distinct light absorption characteristics measured by UV-Vis (**Figure 1**). As shown in **Figure 1A**, Eosin Y absorbs photons strongly in the green light region (the green light irradiation in this study is between 500–570 nm), while exhibiting little or no light absorption in the UV range (the UV light irradiation in this study is between 329–450 nm). In contrast, Omnirad 2100 shows no absorption in the green light region,

while absorbing light strongly in the UV range (**Figure 1B**). The nearly non-overlapping light absorption between Omnirad 2100 and Eosin Y allows them to be used in combination to induce wavelength-selective curing of the thiol-acrylate photoresins in this study. Specifically, under green light irradiation, Eosin Y triggers the TBD-HBPh$_4$ photobase generator (which does not absorb light; **Figure 1A**) to promote the base-catalyzed thiol-acrylate Michael addition reactions; Under UV light irradiation, Omnirad 2100 cleaves to form free radicals, which then promote radical-mediated photopolymerization pathways (**Scheme 1**). **Figure 1C** displays the UV-Vis spectrum of the entire thiol-acrylate photoresin, showing combined characteristics of green-light absorbing Eosin Y and UV-light absorbing Omnirad 2100. Such coordinated light absorption enables these thiol-acrylate photoresins to undergo orthogonal wavelength-selective reactions to form crosslinked photopolymers with distinct network characteristics, including degradability.

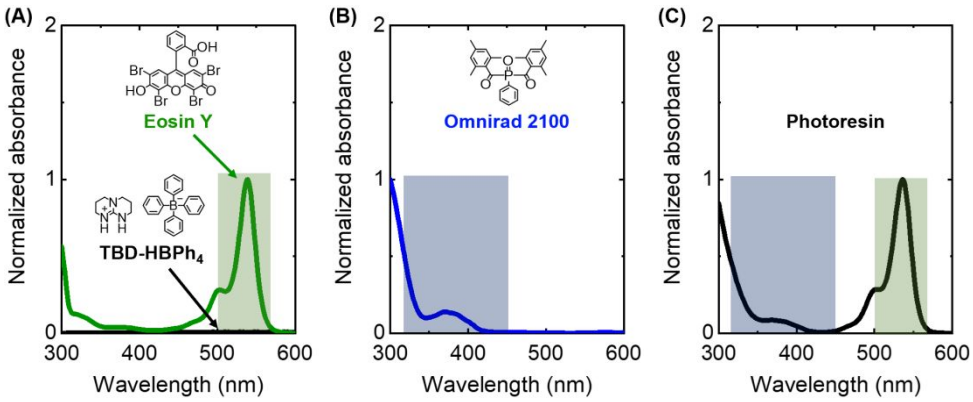

Fig. 1. UV-Vis absorption spectra of **(A)** Eosin Y and TBD-HBPh$_4$, **(B)** Omnirad 2100, and **(C)** photoresin mixture. The shaded regions in **(A)**–**(C)** represent the wavelength ranges of the two light sources employed in this study.

3.1. Curing of thiol-acrylate photoresins under green light irradiation

3.1.1. Curing mechanism and characteristics

Upon green light irradiation, the Eosin Y photosensitizer absorbs photons and transitions from a ground state to an excited state. A photoinduced electron transfer from the borate (BPh_4^-) to the excited Eosin Y occurs subsequently, generating a ketyl radical anion that extracts a proton

from the TBD-H^+ cation to release the strong TBD base **(Figure S3A)**.[54] The resulting TBD base deprotonates thiols to form thiolate anions, which then initiate the anion-mediated thiol-acrylate Michael addition reactions. This will result in a stoichiometric consumption of [SH] and [C=C] functional groups, eventually forming a thiol-acrylate step-growth network crosslinked by dynamic disulfide bonds (**Scheme 1**). It is noteworthy that the intermediates of Eosin Y and TBD-$HBPh_4$ can undergo side reactions to form unwanted free radicals (**Figure S3B**). To ensure that the photoresin solely adopts the anionic thiol-acrylate Michael addition[55] reaction pathway under green light irradiation, TEMPO was added to serve as a radical scavenger to suppress the unwanted radical-mediated reactions (such reactions will be detailed in **Section 3.2** below).[56]

Figure 2 compiles the FTIR spectra of the thiol-acrylate photoresin before and after green light irradiation, both with and without TEMPO. When TEMPO was incorporated into the photoresin, both [SH] and [C=C] groups reached nearly full consumption after green light curing (**Figures 2A** and **2B**), indicating that the photoresin underwent stoichiometric thiol-acrylate Michael addition reactions under such circumstances. In contrast, when TEMPO was not incorporated into the photoresin, [C=C] groups reached nearly full consumption whereas [SH] groups showed minimal consumption (**Figures 2C** and **2D**). This nonstoichiometric consumption of [SH] and [C=C] groups after green light irradiation without TEMPO is likely due to the unwanted radical-mediated reactions (e.g., acrylate homopolymerization; see **Section 3.2** below). Therefore, these results demonstrate the essential role of TEMPO as a radical scavenger in suppressing/eliminating the unwanted free radicals generated during the green-light photoinitiation process, ensuring that the photoresin solely undergoes anionic thiol-acrylate Michael addition reactions in a stoichiometric manner.

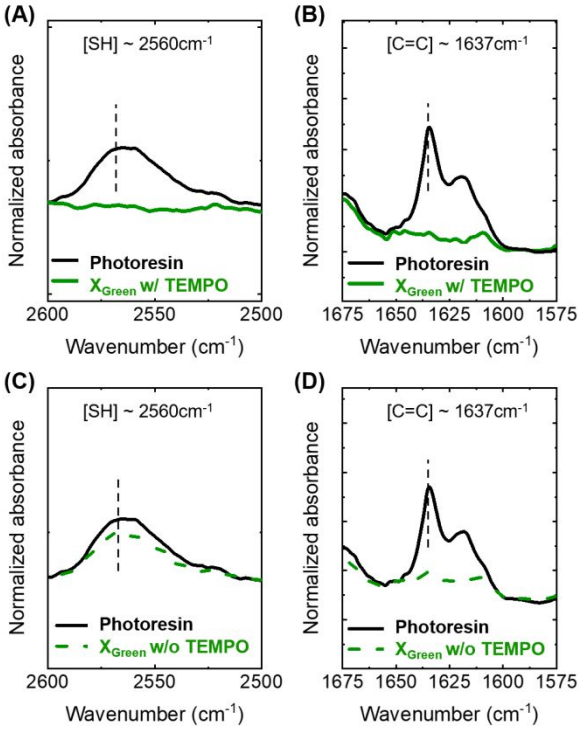

Fig. 2. ATR-FTIR spectra of the thiol-acrylate photoresin before and after green light irradiation at an intensity of 80 mW cm^{-2} for 15 min: (**A**) thiol peak with TEMPO (**B**) acrylate peak with TEMPO, (**C**) thiol peak without TEMPO, and (**D**) acrylate peak without TEMPO.

3.1.2. Material properties of the green-light cured thiol-acrylate photoresins

Crosslinking of the thiol-acrylate photoresins after curing with green light in presence of TEMPO was confirmed by their insolubility and swelling behavior in good solvents. These green light-cured thiol-acrylate photoresins are noted as X_{Green} samples throughout this manuscript, and their material properties are compiled in **Table 1**. Specifically, swelling tests of these X_{Green} samples reported a relatively high gel fraction of ~95 wt%, consistent with the nearly full consumption of both [SH] and [C=C] groups after curing. DSC measurements on these X_{Green} samples reported a glass transition temperature (T_g) of ~ –46 °C and a relatively narrow transition region (i.e., $T_{g,endset}$ - $T_{g,onset}$ ≈ 17 °C; **Figure 3A**). In addition, TGA characterizations of these X_{Green} samples reported a degradation temperature at 5% weight loss ($T_{d,\ 5wt\%}$) of ~219 °C (**Figure 3B**). Furthermore, room-temperature tensile tests of these X_{Green} samples reported a Young's modulus

of ~3.9 MPa, an elongation at break of ~14%, and a tensile strength of ~0.5 MPa (**Figure 3C**).

Table 1. Gel fraction values and thermomechanical properties of X_{Green} and X_{UV} samples.

Sample[a]	X_{Green}	X_{UV}
Gel fraction (wt%)	95.0 ± 0.3	79.0 ± 0.6
T_g (°C)	-46 ± 1	-52 ± 1
$T_{d,\ 5wt\%}$ (°C)	219 ± 3	194 ± 1
Young's modulus[b] [MPa]	3.9 ± 0.1	2.7 ± 0.1
Elongation at break[b] [%]	14.2 ± 0.8	4.8 ± 0.5
Tensile strength[b] [MPa]	0.49 ± 0.03	0.12 ± 0.01

[a]Reported errors are standard deviations from multiple measurements.
[b]Tensile properties measured at room temperature

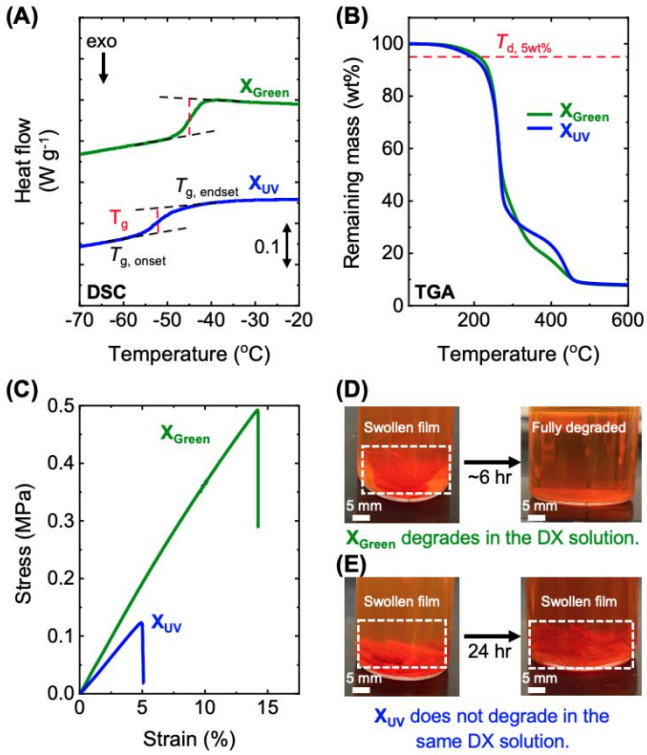

Fig. 3. (**A**) DSC thermograms, (**B**) TGA analyses, and (**C**) room-temperature tensile tests of X_{Green} and X_{UV} samples as well as visual evolution of (**D**) X_{Green} and (**E**) X_{UV} samples after immersion in the decrosslinking solution for 24 h.

More importantly, these X_{Green} samples should contain dynamic disulfide [S-S] bonds within their crosslinking network strands (see **Scheme 1** and **Section 3.1.1**), which allow them to undergo network degradation/deconstruction via thiol-disulfide exchange reactions with reactive thiols (i.e., Thioplast G4) in a basic environment.[48] Consistently, **Figure 3D** visualizes the network

degradation process of these X_{Green} samples in a decrosslinking solution comprised of Thioplast G4, triethylamine base catalyst, and acetone. After immersing for ~6 h, these X_{Green} samples underwent complete network degradation, resulting in a homogeneous solution of soluble decrosslinked materials. (It is worth noting that the degradation rate of this system can be tuned by varying the degradation conditions including temperature and reactive thiol content.[48]) A careful ^{1}H NMR analysis (**Figure S4**) of the resulting decrosslinked materials confirmed the complete X_{Green} network degradation via base-catalyzed thiol-disulfide exchange reactions (see **Supporting Information** for details), in a manner similar to that reported in our previous study.[48] Notably, these decrosslinked materials contain the same amount of [SH] groups as those in the original decrosslinking solution (since [SH] content remains constant after thiol-disulfide exchange), which can be recrosslinked with a stoichiometric amount of triacrylate monomers, if needed.[48]

3.2. Curing of thiol-acrylate photoresins under UV light irradiation

3.2.1. Curing mechanism and characteristics

Upon UV light irradiation, the Omnirad 2100 photoinitiator (Norrish type I[57-59]) undergoes alpha-bond cleavage to generate sufficient free radicals that overcome the radical inhibition effect caused by TEMPO and subsequently react with thiols to form thiyl radicals, thus triggering radical-mediated thiol-acrylate reactions. As shown in **Scheme 1** and reported in previous literature,[26, 27] these thiyl radicals can readily react with [C=C] groups to form carbon-centered radicals, which then undergo either chain transfer reactions with thiols to regenerate thiyl radicals (i.e., thiol-acrylate addition) or competitive chain-growth reactions with [C=C] bonds (i.e., acrylate homopolymerization).[26, 27] The co-existence of these two distinct radical-mediated reaction

pathways would typically result in a non-stoichiometric consumption of [SH] and [C=C] groups.

According to the FTIR spectra shown in **Figures 4A** and **4B**, <50 mol% of the [SH] groups in the thiol-acrylate photoresin were consumed after UV curing at 50 mW cm^{-2} for 6 minutes, whereas the [C=C] groups were almost fully consumed. (Note that the relatively long UV curing time could be attributed to the presence of TEMPO as a radical inhibitor.) **Figure 4C** plots the evolution of [SH] and [C=C] conversion over time during UV light irradiation at an intensity of 50 mW cm^{-2}. As shown in **Figure 4C**, both [SH] and [C=C] conversion increased gradually at almost equal rates with increasing UV irradiation time up to ~2.5 min, indicating that radical-based thiol-acrylate addition reactions dominated initially. After ~2.5 min, both [SH] and [C=C] conversion increased dramatically, with [C=C] conversion exhibiting a much bigger stepwise increase with increasing irradiation time (achieved ~80% [C=C] conversion within ~1.5 min; **Figure 4C**). This indicates that the acrylate homopolymerization contributed to a greater extent to the overall [C=C] conversion during this stage, as compared to the thiol-acrylate addition reaction. This observation is consistent with a previous study by Cramer and Bowman, which reported an acrylate homopolymerization rate constant ~1.5 times greater than the thiol-acrylate addition.[26] Finally, the conversion of [SH] and [C=C] groups leveled after ~5 min of UV irradiation at ~44% and ~97%, respectively. Such a non-stoichiometric functional group consumption confirms the co-existence of radical-mediated acrylate homopolymerization and thiol-acrylate addition reactions.

Figure 4D shows the evolution of storage (G') and loss (G'') shear moduli over time during UV light irradiation at an intensity of 50 mW cm^{-2}. Initially, G' and G'' increased gradually, then G' increased dramatically and exceed G'' after ~2 min of UV irradiation. This crossover is known as the gel point, above which the material transitions from a liquid-like behavior to solid-like behavior.[60, 61] Notably, the gelation process occurred concurrently with a dramatic increase in the

[C=C] conversion (**Figure 4C**), indicative of the chain-growth network formation via acrylate homopolymerization.[26, 62-64] Finally, G' and G'' plateaued after ~6 min of UV irradiation at ~1 MPa and 10 kPa, respectively. Overall, these photo-rheological data are consistent with the FTIR characterizations, both of which demonstrate the co-existence of radical-mediated acrylate homopolymerization and thiol-acrylate addition reactions under UV light irradiation.

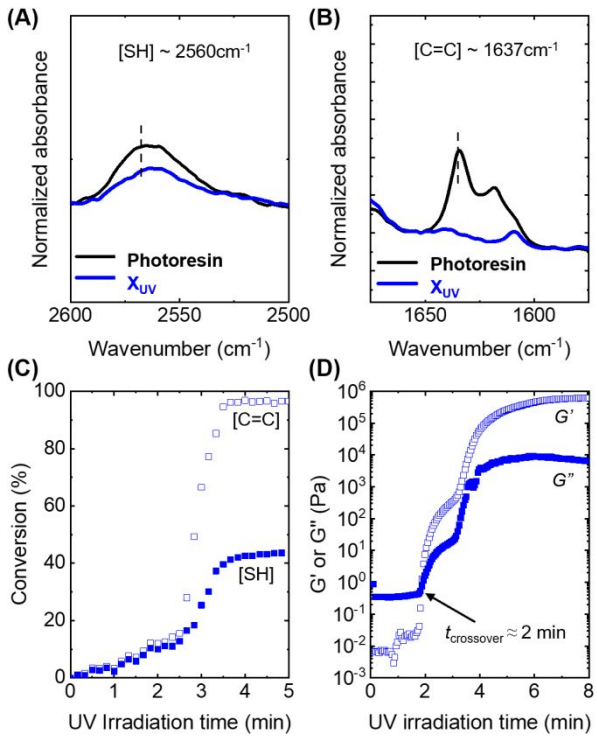

Fig. 4. ATR-FTIR spectra of the thiol-acrylate photoresin before and after UV irradiation at an intensity of 50 mW cm^{-2} for 6 min, highlighting the (**A**) thiol peak and (**B**) acrylate peak; The evolution of (**C**) thiol and acrylate conversion as well as (**D**) G' and G'' with increasing UV irradiation time.

3.2.2. Material properties of the UV-light cured thiol-acrylate photoresins

Crosslinking of the thiol-acrylate photoresins after curing with UV light was also confirmed by their insolubility and swelling behavior in good solvents. These UV light-cured thiol-acrylate photoresins are thus noted as X_{UV} samples throughout this manuscript, and their material

properties are also compiled in **Table 1**. Specifically, swelling tests of these X_{UV} samples reported a gel fraction of ~79 wt% (**Table 1**), consistent with the incomplete conversion of [SH] groups. ^{1}H NMR analysis of the sol fraction of these X_{UV} samples confirmed the presence of unreacted [SH] groups (**Figure S5**), indicating that some Thioplast G4 molecules were not incorporated into the X_{UV} network structures and remained as the soluble fractions that can be extracted out of these X_{UV} samples.

DSC measurements on these X_{UV} samples reported a T_g of ~ –52 °C, ~6 °C lower than that of X_{Green} (**Table 1** and **Figure 3A**). This difference could be attributed to the presence of residual [SH]-containing molecules, which can act as plasticizers to lower the T_g of these X_{UV} samples. Notably, X_{UV} showed a glass transition region (i.e., $T_{g,endset}$ - $T_{g,onset}$ ≈ 30 °C in **Figure 3A**) much broader than that of X_{Green}. This is likely because X_{UV} has a greater network heterogeneity due to its combined chain- and step-growth photopolymerization mechanisms, as compared to the relatively uniform X_{Green} step-growth network.[65] In addition, these X_{UV} samples reported a $T_{d,\ 5wt\%}$ of ~194 °C (**Table 1**), and they exhibited two step-wise weight losses (**Figure 3B**), possibly due to their heterogenous structures comprising strands formed via both acrylate homopolymerization and thiol-acrylate addition reactions. Furthermore, room-temperature tensile tests of these X_{UV} samples reported a Young's modulus of ~2.7 MPa, an elongation at break of ~5%, and a tensile strength of ~0.1 MPa, all of which are slightly lower than those for X_{Green} samples (**Table 1** and **Figure 3C**). (It is noteworthy that the tensile properties of both X_{UV} and X_{Green} samples in this study are relatively poor, and future studies are warranted to improve their mechanical performance by optimizing photoresin formulations.)

When these X_{UV} samples were immersed in the same decrosslinking solution (i.e., Thioplast G4, triethylamine base catalyst, and acetone) that completely degrades the X_{Green}

samples, they only showed swelling behavior without any sign of network degradation after 24 h (**Figure 3D**). This is within expectation because these X_{UV} samples are mainly comprised of permanently crosslinked networks formed by acrylate homopolymerization. Therefore, these X_{UV} samples would remain intact under the same decrosslinking conditions where dynamic X_{Green} networks degrade via thiol-disulfide exchange reactions.

3.3. Patterned curing of thiol-acrylate photoresins & Selective network degradation

As demonstrated in **Sections 3.1** and **3.2** above, the thiol-acrylate photoresins in this study can be selectively cured by green light *vs.* UV light to form a degradable, dynamic network *vs.* a non-degradable, permanent network, respectively. Its unique capability of undergoing orthogonal wavelength-selective reactions renders this thiol-acrylate photoresin suitable for fabricating crosslinked multimaterials with programmed degradability. For demonstration, this thiol-acrylate photoresin was casted between two glass slides with ~0.5-mm-thick spacers, and the resulting assembly was irradiated by the patterned UV light through a photomask with an "ASU" logo or a "butterfly" shape. After patterned UV curing, the whole film (containing both UV-cured and uncured regions) was irradiated with green light (**Figure 5A**). The as-obtained single-layer films appeared visually featureless, and the interface between the green- and UV-light cured regions was not obvious to naked eyes (**Figures 5B** and **5C**). According to SEM characterizations, the as-cured films showed a continuous and relatively smooth surface, without any noticeable interfacial defects between the green- and UV-light irradiated regions (**Figure 5C**).

After selectively degrading the green-light irradiated regions in these single-layer films, discrete holes were created inside the continuous UV-light irradiated pattern, thus revealing the originally hidden "ASU" logo (**Figure 5B**) and the "butterfly" shape (**Figure 5C**). As shown by

SEM, the resulting patterned samples (UV-cured parts) also showed a continuous and relatively smooth surface without any visible defects/cracks (**Figure 5C**). Notably, the new surfaces formed after removing the green-light irradiated regions also appeared relatively smooth. These results demonstrate that these thiol-acrylate photoresins can undergo orthogonal wavelength-selective reactions under patterned green- and UV-light irradiation to form crosslinked multimaterials with pre-designed degradable regions that can be subsequently removed to reveal the underlying photomasks' patterns.

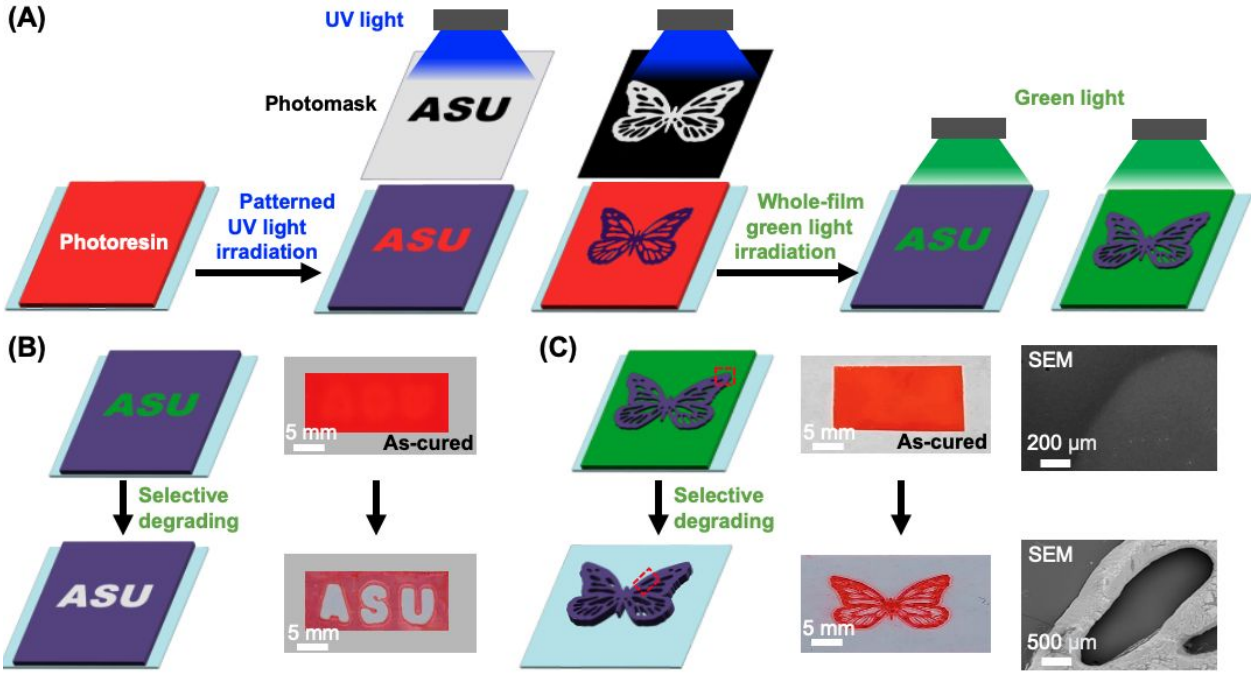

Fig. 5. Curing of the thiol-acrylate photoresin by patterned UV light irradiation through photomasks having (**A**) an "ASU" logo and a "butterfly" shape, followed by whole-film green light irradiation. The visual appearance of the as-cured films from **(A)** with an **(B)** "ASU" logo and **(C)** "butterfly" shape before and after selectively degrading the green-light irradiated regions. SEM images are focused on the regions highlighted by the red boxes in **(C)**.

4. Conclusions

This manuscript described a wavelength-selective photopolymerization process of a new

thiol-acrylate photoresin for fabricating multimaterials that combine both degradable, dynamic and non-degradable, permanent networks. Specifically, green light irradiation triggers photobase generators to catalyze the thiol-acrylate Michael addition reactions, forming a step-growth network that is crosslinked by dynamic disulfide bonds and can thus be degraded or decrosslinked through thiol-disulfide exchange reactions with excess reactive thiols. Meanwhile, UV light irradiation cleaves radical photoinitiators to promote both radical-mediated acrylate homopolymerization and thiol-acrylate addition reactions, forming a permanently crosslinked chain-growth network that cannot be degraded under the same decrosslinking conditions. This wavelength-selective characteristic allows this thiol-acrylate photoresin to undergo orthogonal photopolymerization under patterned green- and UV-light irradiation to form visually featureless crosslinked multimaterials with pre-designed degradable regions. Importantly, these multimaterials can reveal the underlying complex patterns after selectively removing the degradable regions. Overall, the dual-wavelength photoresins demonstrated in this study could not only provide alternative photopatterning material solutions with tunable properties for lithography applications but also help promote the circular sustainability of photopolymers in general. Moreover, it can be extended to facilitate 3D printing of hierarchically structured materials, by either printing degradable support structures that help maintain the shape of the printed objects or printing sacrificial layers that can be degraded to create voids/channels in the printed objects. Currently, our group is exploring other wavelength-selective chemistries (e.g., hybrid thiol-acrylate/epoxy system) to promote the reaction kinetics of these photoresins and enhance the thermomechanical properties of the resulting multimaterials.

ASSOCIATED CONTENT

Supporting Information

^{1}H NMR results and photochemical pathways involving Eosin Y.

AUTHOR INFORMATION

Corresponding Author

Kailong Jin; Email: kailong.jin@asu.edu

AUTHOR CONTRIBUTIONS

Saleh Alfarhan: conceptualization, methodology, validation, writing – original draft, writing – review and editing; Jared Nettles: methodology; Parimal Prabhudesai: methodology; Jen-Chieh Yu: methodology; Clarissa Westover: methodology; Tengteng Tang: methodology; Wenbo Wang: conceptualization; Xiangfan Chen: conceptualization, writing – review and editing; Soyoung E. Seo: writing – review and editing; Xiangjia Li: writing – review and editing; Timothy Long: writing – review and editing; Kailong Jin: conceptualization, validation, funding acquisition, supervision, project administration, writing – review and editing.

CONFLICT OF INTEREST

There are no conflicts of interest to declare.

ACKNOWLEDGMENTS

K. Jin and S. Alfarhan acknowledge the startup research funding support provided by the

Ira A. Fulton Schools of Engineering at Arizona State University (ASU). K. Jin, J. Nettles, C. Westover, and T. Long acknowledge funding support from the National Science Foundation (NSF; grant number: EFRI E3P 2132183). X. Li acknowledges funding support from the NSF (grant number: CMMI 2114119). S. E. Seo and J. Yu acknowledge Ralph E. Powe Junior Faculty Enhancement Award from the ORAU for partial student support. X. Chen and W. Wang acknowledge funding support from the NSF (CMMI 2229279) and the ASU-Mayo Seed Grant.

REFERENCES

1. Hansen, M. J.; Velema, W. A.; Lerch, M. M.; Szymanski, W.; Feringa, B. L., Wavelength-selective cleavage of photoprotecting groups: strategies and applications in dynamic systems. *Chemical Society Reviews* **2015,** *44* (11), 3358-3377.

2. Lu, P.; Ahn, D.; Yunis, R.; Delafresnaye, L.; Corrigan, N.; Boyer, C.; Barner-Kowollik, C.; Page, Z. A., Wavelength-selective light-matter interactions in polymer science. *Matter* **2021,** *4* (7), 2172-2229.

3. Corrigan, N.; Ciftci, M.; Jung, K.; Boyer, C., Mediating Reaction Orthogonality in Polymer and Materials Science. *Angewandte Chemie International Edition* **2021,** *60* (4), 1748-1781.

4. Chatani, S.; Kloxin, C. J.; Bowman, C. N., The power of light in polymer science: photochemical processes to manipulate polymer formation, structure, and properties. *Polymer Chemistry* **2014,** *5* (7), 2187-2201.

5. Corrigan, N.; Boyer, C., 100th Anniversary of Macromolecular Science Viewpoint: Photochemical Reaction Orthogonality in Modern Macromolecular Science. *ACS Macro Letters* **2019,** *8* (7), 812-818.

6. Stanton-Humphreys, M. N.; Taylor, R. D.; McDougall, C.; Hart, M. L.; Brown, C. T.; Emptage, N. J.; Conway, S. J., Wavelength-orthogonal photolysis of neurotransmitters in vitro. *Chem Commun (Camb)* **2012,** *48* (5), 657-9.

7. Leung, S. J.; Kachur, X. M.; Bobnick, M. C.; Romanowski, M., Wavelength-Selective Light-Induced Release from Plasmon Resonant Liposomes. *Adv Funct Mater* **2011,** *21* (6), 1113-1121.

8. Carioscia, J. A.; Stansbury, J. W.; Bowman, C. N., Evaluation and control of thiol–ene/thiol–epoxy hybrid networks. *Polymer* **2007,** *48* (6), 1526-1532.

9. Yu, B.; Zheng, J.; Wu, J.; Ma, H.; Zhou, X.; Hui, Y.; Liu, F.; He, J., Preparation of isotropic tensile photosensitive resins for digital light processing 3D printing using orthogonal thiol-ene and thiol-epoxy dual-cured strategies. *Polymer Testing* **2022,** *116*, 107767.

10. Grauzeliene, S.; Navaruckiene, A.; Skliutas, E.; Malinauskas, M.; Serra, A.; Ostrauskaite, J., Vegetable oil-based thiol-ene/thiol-epoxy resins for laser direct writing 3D micro-/nano-lithography. *Polymers* **2021,** *13* (6), 872.

11. Oxman, J. D.; Jacobs, D. W.; Trom, M. C.; Sipani, V.; Ficek, B.; Scranton, A. B., Evaluation of initiator systems for controlled and sequentially curable free-radical/cationic hybrid photopolymerizations. *Journal of Polymer Science Part A: Polymer Chemistry* **2005,** *43* (9), 1747-1756.

12. Dolinski, N. D.; Page, Z. A.; Callaway, E. B.; Eisenreich, F.; Garcia, R. V.; Chavez, R.; Bothman, D. P.; Hecht, S.; Zok, F. W.; Hawker, C. J., Solution Mask Liquid Lithography (SMaLL) for One-Step, Multimaterial 3D Printing. *Advanced Materials* **2018,** *30* (31), 1800364.

13. Schwartz, J. J.; Boydston, A. J., Multimaterial actinic spatial control 3D and 4D printing. *Nature Communications* **2019,** *10* (1), 791.

14. Dolinski, N. D.; Callaway, E. B.; Sample, C. S.; Gockowski, L. F.; Chavez, R.; Page, Z. A.; Eisenreich, F.; Hecht, S.; Valentine, M. T.; Zok, F. W.; Hawker, C. J., Tough Multimaterial Interfaces through Wavelength-Selective 3D Printing. *ACS Applied Materials & Interfaces* **2021,** *13* (18), 22065-22072.

15. Cazin, I.; Gleirscher, M. O.; Fleisch, M.; Berer, M.; Sangermano, M.; Schlögl, S., Spatially controlling the mechanical properties of 3D printed objects by dual-wavelength vat photopolymerization. *Additive Manufacturing* **2022,** *57*, 102977.

16. Nair, D. P.; Cramer, N. B.; Gaipa, J. C.; McBride, M. K.; Matherly, E. M.; McLeod, R. R.; Shandas, R.; Bowman, C. N., Two-Stage Reactive Polymer Network Forming Systems. *Advanced Functional Materials* **2012,** *22* (7), 1502-1510.

17. Zhang, X.; Xi, W.; Huang, S.; Long, K.; Bowman, C. N., Wavelength-Selective Sequential Polymer Network Formation Controlled with a Two-Color Responsive Initiation System. *Macromolecules* **2017,** *50* (15), 5652-5660.

18. Zhang, X.; Cox, L.; Wen, Z.; Xi, W.; Ding, Y.; Bowman, C. N., Implementation of two distinct wavelengths to induce multistage polymerization in shape memory materials and nanoimprint lithography. *Polymer* **2018,** *156*, 162-168.

19. Konuray, A. O.; Liendo, F.; Fernández-Francos, X.; Serra, À.; Sangermano, M.; Ramis, X., Sequential curing of thiol-acetoacetate-acrylate thermosets by latent Michael addition reactions. *Polymer* **2017,** *113*, 193-199.

20. Jian, Y.; He, Y.; Sun, Y.; Yang, H.; Yang, W.; Nie, J., Thiol–epoxy/thiol–acrylate hybrid materials synthesized by photopolymerization. *Journal of Materials Chemistry C* **2013,** *1* (29), 4481-4489.

21. Shin, J.; Matsushima, H.; Comer, C. M.; Bowman, C. N.; Hoyle, C. E., Thiol−Isocyanate−Ene Ternary Networks by Sequential and Simultaneous Thiol Click Reactions. *Chemistry of Materials* **2010,** *22* (8), 2616-2625.

22. Rossegger, E.; Strasser, J.; Höller, R.; Fleisch, M.; Berer, M.; Schlögl, S., Wavelength Selective Multi-Material 3D Printing of Soft Active Devices Using Orthogonal Photoreactions. *Macromolecular Rapid Communications* **2023,** *44* (2), 2200586.

23. Hoekstra, D. C.; van der Lubbe, B. P. A. C.; Bus, T.; Yang, L.; Grossiord, N.; Debije, M. G.; Schenning, A. P. H. J., Wavelength-Selective Photopolymerization of Hybrid Acrylate-Oxetane Liquid Crystals. *Angewandte Chemie International Edition* **2021,** *60* (19), 10935-10941.

24. Foster, J. C.; Cook, A. W.; Monk, N. T.; Jones, B. H.; Appelhans, L. N.; Redline, E. M.; Leguizamon, S. C., Continuous Additive Manufacturing using Olefin Metathesis. *Advanced Science* **2022,** *9* (14), 2200770.

25. Kaupp, M.; Hiltebrandt, K.; Trouillet, V.; Mueller, P.; Quick, A. S.; Wegener, M.; Barner-Kowollik, C., Wavelength selective polymer network formation of end-functional star polymers. *Chemical Communications* **2016,** *52* (9), 1975-1978.

26. Cramer, N. B.; Bowman, C. N., Kinetics of thiol–ene and thiol–acrylate photopolymerizations with real-time fourier transform infrared. *Journal of Polymer Science Part A: Polymer Chemistry* **2001,** *39* (19), 3311-3319.

27. Lecamp, L.; Houllier, F.; Youssef, B.; Bunel, C., Photoinitiated cross-linking of a thiol–methacrylate system. *Polymer* **2001,** *42* (7), 2727-2736.

28. Konuray, A. O.; Fernández-Francos, X.; Ramis, X., Curing kinetics and characterization of dual-curable thiol-acrylate-epoxy thermosets with latent reactivity. *Reactive and Functional Polymers* **2018,** *122*, 60-67.

29. Ma, Y.; Kottisch, V.; McLoughlin, E. A.; Rouse, Z. W.; Supej, M. J.; Baker, S. P.; Fors, B. P., Photoswitching Cationic and Radical Polymerizations: Spatiotemporal Control of Thermoset Properties. *Journal of the American Chemical Society* **2021,** *143* (50), 21200-21205.

30. Chen, Q.; Yang, Q.; Gao, P.; Chi, B.; Nie, J.; He, Y., Photopolymerization of Coumarin-Containing Reversible Photoresponsive Materials Based on Wavelength Selectivity. *Industrial & Engineering Chemistry Research* **2019,** *58* (8), 2970-2975.

31. Truong, V. X.; Li, F.; Ercole, F.; Forsythe, J. S., Wavelength-Selective Coupling and Decoupling of Polymer Chains via Reversible [2 + 2] Photocycloaddition of Styrylpyrene for Construction of Cytocompatible Photodynamic Hydrogels. *ACS Macro Letters* **2018,** *7* (4), 464-469.

32. Rylski, A. K.; Cater, H. L.; Mason, K. S.; Allen, M. J.; Arrowood, A. J.; Freeman, B. D.; Sanoja, G. E.; Page, Z. A., Polymeric multimaterials by photochemical patterning of crystallinity. *Science* **2022,** *378* (6616), 211-215.

33. Allen, M. J.; Lien, H.-M.; Prine, N.; Burns, C.; Rylski, A. K.; Gu, X.; Cox, L. M.; Mangolini, F.; Freeman, B. D.; Page, Z. A., Multimorphic Materials: Spatially Tailoring Mechanical Properties via Selective Initiation of Interpenetrating Polymer Networks. *Advanced Materials* **2023,** *35* (9), 2210208.

34. Nair, D. P.; Podgórski, M.; Chatani, S.; Gong, T.; Xi, W.; Fenoli, C. R.; Bowman, C. N., The Thiol-Michael Addition Click Reaction: A Powerful and Widely Used Tool in Materials Chemistry. *Chemistry of Materials* **2014,** *26* (1), 724-744.

35. Konuray, O.; Fernández-Francos, X.; Ramis, X.; Serra, À., State of the Art in Dual-Curing Acrylate Systems. *Polymers* **2018,** *10* (2), 178.

36. Huang, S.; Kong, X.; Xiong, Y.; Zhang, X.; Chen, H.; Jiang, W.; Niu, Y.; Xu, W.; Ren, C., An overview of dynamic covalent bonds in polymer material and their applications. *European Polymer Journal* **2020,** *141*, 110094.

37. Wojtecki, R. J.; Meador, M. A.; Rowan, S. J., Using the dynamic bond to access macroscopically responsive structurally dynamic polymers. *Nature Materials* **2011,** *10* (1), 14-27.

38. Chakma, P.; Konkolewicz, D., Dynamic Covalent Bonds in Polymeric Materials. *Angewandte Chemie International Edition* **2019,** *58* (29), 9682-9695.

39. Scheutz, G. M.; Lessard, J. J.; Sims, M. B.; Sumerlin, B. S., Adaptable Crosslinks in Polymeric Materials: Resolving the Intersection of Thermoplastics and Thermosets. *Journal of the American Chemical Society* **2019,** *141* (41), 16181-16196.

40. Zheng, N.; Xu, Y.; Zhao, Q.; Xie, T., Dynamic Covalent Polymer Networks: A Molecular Platform for Designing Functions beyond Chemical Recycling and Self-Healing. *Chemical Reviews* **2021,** *121* (3), 1716-1745.

41. McBride, M. K.; Worrell, B. T.; Brown, T.; Cox, L. M.; Sowan, N.; Wang, C.; Podgorski, M.; Martinez, A. M.; Bowman, C. N., Enabling Applications of Covalent Adaptable Networks. *Annual Review of Chemical and Biomolecular Engineering* **2019,** *10* (1), 175-198.

42. Musgrave, G. M.; Bishop, K. M.; Kim, J. S.; Heiner, A. C.; Wang, C., Polyester networks from structurally similar monomers: recyclable-by-design and upcyclable to photopolymers. *Polymer Chemistry* **2023,** *14* (25), 2964-2970.

43. Jin, K.; Li, L.; Torkelson, J. M., Recyclable Crosslinked Polymer Networks via One-Step Controlled Radical Polymerization. *Advanced Materials* **2016,** *28* (31), 6746-6750.

44. Dobbins, D. J.; Scheutz, G. M.; Sun, H.; Crouse, C. A.; Sumerlin, B. S., Glass-transition temperature governs the thermal decrosslinking behavior of Diels–Alder crosslinked polymethacrylate networks. *Journal of Polymer Science* **2020,** *58* (1), 193-203.

45. Choi, C.; Okayama, Y.; Morris, P. T.; Robinson, L. L.; Gerst, M.; Speros, J. C.; Hawker, C. J.; Read de Alaniz, J.; Bates, C. M., Digital Light Processing of Dynamic Bottlebrush Materials. *Advanced Functional Materials* **2022,** *32* (25), 2200883.

46. Catt, S. O.; Long, T. E.; Blasco, E.; Sardon, H., Loop 3D printing: recyclable photoresins for light-mediated additive manufacturing. **2023**.

47. Kuenstler, A. S.; Hernandez, J. J.; Trujillo-Lemon, M.; Osterbaan, A.; Bowman, C. N., Vat Photopolymerization Additive Manufacturing of Tough, Fully Recyclable Thermosets. *ACS Applied Materials & Interfaces* **2023,** *15* (8), 11111-11121.

48. Alfarhan, S.; Brown, J.; Liu, B.; Long, T.; Jin, K., Chemically recyclable crosslinked thiol-ene photopolymers via thiol-disulfide exchange reactions. *Journal of Polymer Science* **2022,** *60* (24), 3379-3390.

49. Zhou, L.; Chen, M.; Zhao, X., Rapid degradation of disulfide-based thermosets through thiol-disulfide exchange reaction. *Polymer* **2017,** *120*, 1-8.

50. Fernandes, P. A.; Ramos, M. J., Theoretical insights into the mechanism for thiol/disulfide exchange. *Chemistry* **2004,** *10* (1), 257-66.

51. Brown, J. R.; Herzberger, J.; Spiering, G. A.; Wilts, E.; Moore, R. B.; Long, T. E., Binary Thiol-Acrylate Photopolymerization for the Design of Degradable Acetal-Functionalized Hydrogels. *ACS Applied Polymer Materials* **2023,** *5* (1), 1030-1036.

52. Sun, X.; Gao, J. P.; Wang, Z. Y., Bicyclic Guanidinium Tetraphenylborate: A Photobase Generator and A Photocatalyst for Living Anionic Ring-Opening Polymerization and Cross-Linking of Polymeric Materials Containing Ester and Hydroxy Groups. *Journal of the American Chemical Society* **2008,** *130* (26), 8130-8131.

53. Sharma, L.; Kimura, T., FT-IR Investigation into the miscible interactions in new materials for optical devices. *Polymers for Advanced Technologies* **2003,** *14* (6), 392-399.

54. Trinh, T. K. H.; Morlet-Savary, F.; Pinaud, J.; Lacroix-Desmazes, P.; Reibel, C.; Joyeux, C.; Le Nouen, D.; Métivier, R.; Brosseau, A.; Héroguez, V.; Chemtob, A., Photoreduction of triplet thioxanthone derivative by azolium tetraphenylborate: a way to photogenerate N-heterocyclic carbenes. *Physical Chemistry Chemical Physics* **2019,** *21* (31), 17036-17046.

55. Mather, B. D.; Viswanathan, K.; Miller, K. M.; Long, T. E., Michael addition reactions in macromolecular design for emerging technologies. *Progress in Polymer Science* **2006,** *31* (5), 487-531.

56. Chatani, S.; Gong, T.; Earle, B. A.; Podgórski, M.; Bowman, C. N., Visible-Light Initiated Thiol-Michael Addition Photopolymerization Reactions. *ACS Macro Letters* **2014,** *3* (4), 315-318.

57. Albini, A., Norrish' type I and II reactions and their role in the building of photochemical science. *Photochem Photobiol Sci* **2021,** *20* (1), 161-181.

58. Kirkbride, F. W.; Norrish, R. G. W., The photochemical properties of the carbonyl group. *Transactions of the Faraday Society* **1931,** *27* (0), 404-408.

59. Norrish, R. G. W.; Bamford, C. H., Photo-decomposition of Aldehydes and Ketones. *Nature* **1937,** *140* (3535), 195-196.

60. Chambon, F.; Winter, H. H., Stopping of crosslinking reaction in a PDMS polymer at the gel point. *Polymer Bulletin* **1985,** *13*, 499-503.

61. Jin, K.; Kim, S.-s.; Xu, J.; Bates, F. S.; Ellison, C. J., Melt-Blown Cross-Linked Fibers from Thermally Reversible Diels–Alder Polymer Networks. *ACS Macro Letters* **2018,** *7* (11), 1339-1345.

62. Kury, M.; Ehrmann, K.; Gorsche, C.; Dorfinger, P.; Koch, T.; Stampfl, J.; Liska, R., Regulated acrylate networks as tough photocurable materials for additive manufacturing. *Polymer International* **2022,** *71* (7), 897-905.

63. Senyurt, A. F.; Wei, H.; Phillips, B.; Cole, M.; Nazarenko, S.; Hoyle, C. E.; Piland, S. G.; Gould, T. E., Physical and Mechanical Properties of Photopolymerized Thiol−Ene/Acrylates. *Macromolecules* **2006,** *39* (19), 6315-6317.

64. Okay, O.; Bowman, C. N., Kinetic Modeling of Thiol-Ene Reactions with Both Step and Chain Growth Aspects. *Macromolecular Theory and Simulations* **2005,** *14* (4), 267-277.

65. Sahin, M.; Ayalur-Karunakaran, S.; Manhart, J.; Wolfahrt, M.; Kern, W.; Schlögl, S., Thiol-Ene versus Binary Thiol–Acrylate Chemistry: Material Properties and Network Characteristics of Photopolymers *Advanced Engineering Materials* **2017,** *19* (4), 1600620.